IJRCS

International Journal of Robotics and Control Systems
Vol. 4, No. 4, 2024, pp. 1947-1966
ISSN 2775-2658
http://pubs2.ascee.org/index.php/ijrcs

ASCEE

Nonlinear Model Predictive Control of a Magnetic Levitation System Using Artificial Protozoa Optimizer

Mohanad N. Noaman [a,1,*], Abdurahman Basil Ayoub [a,2], Saif S. Mahmood [a,3]

[a] Department of Systems and Control Engineering, Ninevah University, Ninevah, 41001, Iraq
[1] mohanad.noaman@uoninevah.edu.iq; [2] abdulrahman.ayoub@uoninevah.edu.iq; [3] saif.mahmood@uoninevah.edu.iq
* Corresponding Author

ARTICLE INFO

Article history
Received October 02, 2024
Revised October 27, 2024
Accepted November 12, 2024

Keywords
Maglev Systems;
Nonlinear Model Predictive;
Artificial Protozoa Optimizer;
LQR;
PID

ABSTRACT

A magnetic levitation system (Maglev) is a sensitive, multi-parameter, nonlinear, and unstable system that is utilized to levitate a ferromagnetic object in free space. Due to its vast applications, various research studies in the field of control strategy have become extremely important and challenging. This work proposes the design of a nonlinear model predictive (NMPC) control scheme for the object position control against the nonlinearities and uncertainties of a Maglev system. A novel bio-inspired Artificial Protozoa Optimization (APO) algorithm is used to fine-tune the NMPC parameters, which include best weighting matrices (Q, R), shorter prediction horizons (N), and shorter time steps (T_P) to minimize the objective cost function. The effective performance of the NMPC is verified using simulation-based results in MATLAB. The CasADi toolbox is utilized to solve nonlinear optimization problems and handle the nonlinearity of the Maglev system model. Simulations are implemented for three trajectories tracking (step, sine, and square) with 20% and without Maglev parameters perturbations. To prove the superiority of the proposed controller, comparisons are made with the conventional Linear Quadratic Regulator (LQR) and proportional-integral-derivative (PID) controllers. Two performance indices are introduced, Integral of Squared Error (ISE) and Integral of Absolute Error (IAE), to examine the tracking performances of the NMPC, LQR, and PID controller. The NMPC controller has shown more efficient performance and accurate results than other controllers. The contributions of this work include a new optimization technique of APO, a new engineering application of the APO integrated with NMPC to control a Maglev system, consideration of inherent nonlinearities and system constraints, and robustness improvement under perturbation.

1. Introduction

A Magnetic Levitation System is characterized by the suspension of an object through the utilization of a magnetic field and the counteraction of gravitational force. The application of the Maglev system is highly relevant in various engineering sectors, including the Maglev trains operating in high speed, wind tunnel levitation models, the use of contactless bearings, disease diagnostics, as well as in suspension and manipulation [1]-[5]. The extensive adoption of the Maglev system can be attributed to its ability to eliminate physical contact between moving and stationary components, effectively addressing friction issues and mitigating vibrations. Consequently,

the Maglev system provides several benefits, such as enabling operation in high vacuum environments, reducing noise levels, and offering a highly precise positioning system [6]. By leveraging the principles of electromagnetism, the Maglev system achieves the levitation of ferromagnetic objects at specific locations within the air space [7]-[10].

The Maglev systems are categorized based on the nature of the magnetic forces, which can be either attractive or repulsive Maglev systems. Designing controllers for such systems is challenging due to their sensitivity, instability, nonlinearity, and the presence of uncertainties [11]. To cope with such issues, various research studies have been done on suitable control techniques to control the position of the levitated object of Maglev systems to enhance dynamic system response.

Different linear and nonlinear controllers such as vision-based [12], [13] and PID be applied to control the Maglev system. However, it is challenging to determine the controllers' parameters without an optimization method which makes the Maglev system stable. In [14], the Harris Hawks (HHO) optimizer-based PID controller is proposed for the unstable Maglev system. Both one Degree of Freedom (1DOF) and two Degrees of Freedom (2DOF) PID controllers are considered to enhance system performance. The research in [15] compares the response of conventional PID and PID-P controllers, focusing on transient response and steady-state details, while the tuning parameters of PID-P controller are optimized by both Particle swarm optimization (PSO) and Black window optimization (BWO) algorithms. However, using PID may not fully capture the complexities of the highly nonlinear nature of magnetic levitation systems. This is due to its sensitivity to parameter changes, tuning complexity, and nonlinear behavior of maglev systems. Linear Quadratic Regulator (LQR) control has been effectively applied to Maglev Systems. LQR with state feedback controller is introduced in [16] for position controlling of steel-ball. [17] introduces an Integral Linear Quadratic Regulator (ILQR) integrated with a proportional gain to achieve robust linearization control of a Maglev System, thereby guaranteeing stability and precise set-point tracking. The performance of the LQR controller is enhanced using PSO optimization in [18] minimizing the time of reaching the desired point. However, LQR relies heavily on an accurate model of the system with limited nonlinearity handling and may not work with constraints. Other linear controllers are frequently tested on a Maglev system such as sliding mode control (SMC) in [19]-[21]. However, chattering is a main drawback of the SMC effect resulting from discontinuous control. A fuzzy controller is utilized in [22]-[24]. Nevertheless, the limitation of fuzzy logic systems lies in the difficulty of optimizing fuzzy controls' parameters, including the selection of membership function types and the number of rules. And linear MPC control strategy is used in [25]-[30]. However, linear controllers often struggle with uncertainties in system models. They may not adequately compensate for variations or unexpected changes in the system. Alongside these controllers, many optimization methods were crucial and implemented for tuning controllers' parameters and finding optimal solution such as particle swarm optimization [31], manta ray foraging optimization [32], atom search optimization [33], and salp swarm algorithm [34].

To address these challenges, this paper proposes a nonlinear model predictive controller (NMPC) for the Maglev system due to its ability to cope with physical system constraints and multivariable interactions and provide a determinable quality of closed-loop behavior. MPC is a modern control technique that uses an internal model and the current measurements to predict the future behavior of the system [35]. MPC is capable of controlling all outputs simultaneously with consideration for input-output interactions. The basic concept of MPC is to use an explicit model to predict the system's future behavior, and then continuously compute a set of control signals by utilizing an optimization algorithm that minimizes the difference between the desired reference trajectory and the predicted system trajectory within a predetermined time horizon [36]-[38]. The use of linearized models in MPC design to offer trajectory tracking or point stabilization for the Maglev system is discussed by the authors of the papers in [39], [40]. By using these methods, the control problem is reduced to a set of simple, fast, and dependable matrix algebra computations. The main disadvantage of using such linearized models for highly nonlinear plants close to an operational point is that they are not accurate enough for changed operating conditions. The insufficient accuracy of MPC with linearized models is

addressed by using nonlinear models in the control application, NMPC, however, this can raise computing costs [41].

To avoid this, the selection of NMPC parameters is critical to the design's effectiveness, particularly when applying NMPC to dynamic systems such as the Maglev system, as these parameters have a great impact on stability, reaction time, control effort, and computational load. The performance of NMPC is significantly influenced by its parameters, such as the prediction horizon (N), time step ΔT, tracking error weighting factor (Q), and control input weighting factor (R). Using three reference trajectories (step, sine, and square), the NMPC scheme is evaluated in comparison to LQR and PID controllers. To provide a fair comparison, the NMPC, LQR, and PID controllers' parameters are optimized using the artificial protozoa optimizer (APO). The APO optimization method, a bio-inspired metaheuristic optimization algorithm, is employed to deal with the complexity of manually tuning the controllers' gains due to its nonlinearity. The APO imitates the survival mechanisms of protozoa behaviors such as foraging, dormancy, and reproduction to enhance optimization processes [42]. The importance of using the APO algorithm is because of its features such as the ability to manage nonlinear optimization problems, balanced exploration and exploitation which is crucial for improving solution quality over iterations, it outperforms many state-of-the-art algorithms, ease of implementation, and robustness in convergence. An evaluation of the proposed approach is conducted using a simulation that utilizes the Interior Point OPTimizer (IPOPT) solver [43] and the CasADi Toolbox [44]-[46] in MATLAB R2023a. The main contribution of this study is listed as follows:

- A novel integration of APO with NMPC.
- Introducing a novel engineering application of APO.
- Inherent nonlinearities consideration of the Maglev system by designing an NMPC under constraints.
- Improvement in system stability and transient response over traditional linear controllers under perturbation.

NMPC is particularly well-suited for Maglev systems because of its ability to handle the system's inherent nonlinearities and the strict constraints required for safe and stable operation. Unlike traditional control methods such as PID or LQR, NMPC excels in managing dynamic uncertainties, such as fluctuating magnetic forces and changes in load or environmental conditions, by constantly updating its control strategy in real-time. As a result, NMPC not only enhances stability but also improves the overall safety and energy efficiency of Maglev systems, making it a more robust solution compared to conventional control approaches.

The rest of this paper is organized as follows: Section 2 highlights the modeling of the Maglev system. Sections 2 illustrate the proposed controller with optimization method. Section 3 discusses the results of the simulation. Section 4 indicates the conclusion of this work by highlighting the future work.

2. Methodology

2.1. Mathematical Modeling of the Maglev System

A Maglev system's schematic representation is displayed in Fig. 1. Using electromagnetic forces, Maglev can be characterized as the ability to levitate an object in the airspace without contact with a solid substance. State equations derived from fundamental physical laws for a ball (sphere) motion in an electromagnetic field can characterize the nonlinear physical model of the Maglev.

$$T = \frac{1}{2}m\dot{x}^2\frac{1}{2}L(x)\dot{q}^2 + \frac{1}{2}\int_0^t R\,\dot{q}^2 dt + mgx + qu$$

where uIs the voltage, $I = \dot{q}$ is the coil's current, R is the coil's resistance, q is the electric charge, and m is the ball's mass. Additionally, g is the gravitational constant, x indicates the ball's distance from the electromagnet, and $L(x)$ is a function that defines the coil inductance's dependency on x. The Lagrangian equations must be satisfied by the variables $q(t)$ and $x(t)$:

$$\frac{d}{dt}\frac{dT}{d\dot{x}} - \frac{\partial T}{\partial x} = 0 \text{ and } \frac{d}{dt}\frac{dT}{d\dot{q}} - \frac{\partial T}{\partial q} = 0$$

which yield

$$\frac{d^2x}{dt^2} = \frac{1}{2m}\frac{dL}{dx}I^2 + g \tag{1}$$

$$\frac{dI}{dt} = \frac{1}{L}\left(-\frac{dL}{dx}\frac{dx}{dt}I - RI + u\right) \tag{2}$$

According to Newton's second law, the equation (1) gives the electromagnetic force as:

$$F(x, I) = \frac{1}{2}\frac{dL}{dx}I^2$$

Polynomial or exponential functions can be used to approximate the coil inductance's dependence on distance:

$$L(x) = L_0 + L_1 e^{-ax} \quad a > 0$$
$$L(x) = L_0 + \frac{1}{a_n x^n + a_{n-1}x^{n-1} + \cdots + a_1 x^1 + a_0} \tag{3}$$

$n \geq 1,\ a_0, \ldots, a_n \in R$

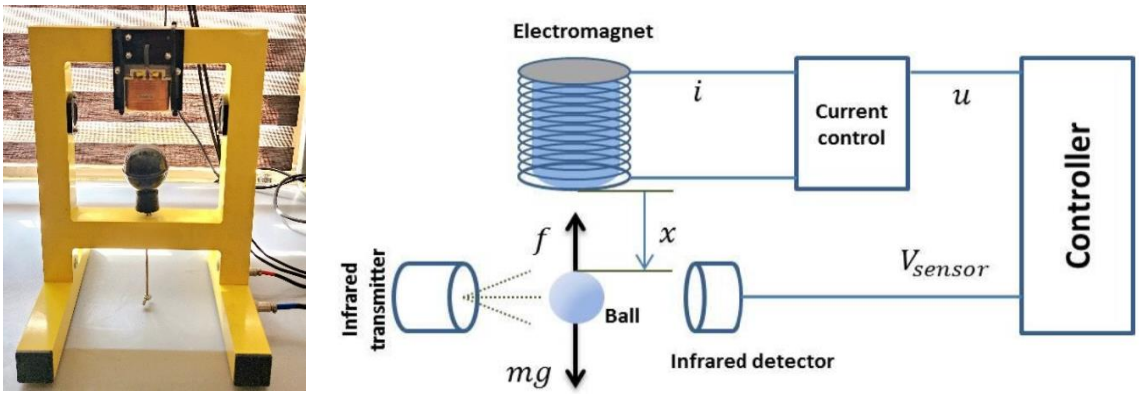

Fig. 1. Magnetic levitation system

Ball dynamics and electromagnetic forces are described using the Lagrange function, which is the difference between kinetic and potential energy and may be expressed as:

The exponential term of (3) is used by having:

$$\frac{dL}{dx} = -aL_1 e^{-ax} \tag{4}$$

where $a \approx \frac{1}{F_{emP2}}$, $L_1 \approx F_{emP1}$ and $\frac{dL}{dx} \approx -\frac{F_{emP1}}{F_{emP2}} e^{-\left(\frac{x_1}{F_{emP2}}\right)}$.

The approximation obtained by experimentation simplifies the equation (2) into:

$$\frac{dI}{dt} = -\frac{1}{f(x)}(ku + c - I) \tag{5}$$

Where $f(x)$ has the same structure as equation (4). By combining (1), (2), (4), and (5), introducing state variables as follows:

$x_1 = x$ is the ball position

$x_2 = \dot{x}$ is the ball velocity

$x_3 = I$ is the current of the coil

The augmented state vector is written as:

$$\mathbf{x} = [x_1, x_2, x_3] \in \mathbb{R}^3$$

With slightly different notation, the following is the formulation of the resulting nonlinear mathematical model:

$$\begin{aligned} \dot{x_1} &= \dot{x} \\ \dot{x_2} &= -\frac{F_{em1}}{2m} + g \\ \dot{x_3} &= \frac{1}{f_i(x_i)}(k_i u + c_i - I) \end{aligned} \tag{6}$$

where $F_{em1} = I^2 \frac{F_{emP1}}{F_{emP2}} e^{-\left(\frac{x}{F_{emP2}}\right)}$, and $f_i(x_i) = \frac{f_{iP1}}{f_{iP2}} e^{-\left(\frac{x}{f_{iP2}}\right)}$.

The reference state vector $\mathbf{x}_r = [x_r \; \dot{x}_r \; I_r]^T \in \mathbb{R}^3$

The output vector of the Maglev system is the ball position:

$$\mathbf{y} = [x] \in \mathbb{R}^1$$

All parameters are summarized in Table 1. Table 1 lists the considered Maglev values for F_{emP1}, F_{emP2}, f_{iP1}, f_{iP2}, k_i, and c_i. These values are particular to the concrete coil and are inherent plant factors. More details can be seen in [47], [48].

Having formulated the system's mathematical foundation, the NMPC will be designed next to address the specific control challenges.

2.2. Nonlinear Model Predictive Control (NMPC) Design

NMPC refers to an MPC controller that utilizes Maglev nonlinear mathematical models for prediction and considering both non-quadratic cost functionals and nonlinear constraints on the process variables [49]. With this prediction feature, optimum control problems can be solved online under limitations on the states, outputs, and inputs. In this context, through a finite horizon, the control input and the error between the reference and the output of the ball position of the Maglev system are minimized. An optimum control sequence is created by the optimization process, in which the system only takes input from the first element in the sequence. Consequently, after shifting the horizon, the same optimization process is repeated at the next sample interval. This procedure known as Receding Horizon Control (RHC) is mostly utilized for compensating for unmeasurable disturbances and modeling errors that cause the system outputs to vary from the predictions of the nonlinear model. The following nonlinear differential equation describes a class of systems for which the stabilization problem is considered:

$$\dot{\mathbf{x}}(t) = \boldsymbol{f}\big(\mathbf{x}(t), \mathbf{u}(t)\big), \quad \mathbf{x}(0) = \mathbf{x}_0 \tag{7}$$

Where The vector field $\boldsymbol{f}: \mathbb{R}^3 \times \mathbb{R}^1 \to \mathbb{R}^3$ is continuous and satisfies $\boldsymbol{f}(\mathbf{0}, \mathbf{0}) = \mathbf{0}$. $\mathbf{x}(t) \in \mathcal{X} \subseteq \mathbb{R}^3$ and $\mathbf{u}(t) \in \mathcal{U} \subseteq \mathbb{R}^1$ denotes the vector of states and inputs, respectively.

Table 1. Maglev parameters values

Name	Parameters	Values	Units
Mass of the ball	m	0.02855	Kg
Gravitational constant	g	9.8100	m/s^2
Electromagnetic force generated by coil 1	F_{emP1}	1.7521×10^{-2}	H
Electromagnetic force generated by coil 2	F_{emP2}	5.8231×10^{-3}	m
Maglev constant	f_{iP1}	1.4142×10^{-4}	$m.s$
Maglev constant	f_{iP2}	4.5626×10^{-3}	m
Control voltage to coil current gain	k_i	2.5165	A/V
Maglev Constant	c_i	0.0243	A
Upper position bound	x_{MAX}	0.0200	m
Minimum coil current	I_{MIN}	0.0388	A
Maximum coil current	I_{MAX}	2.345	A
Minimum Voltage level of control input	U_{MIN}	0.0	V
Maximum Voltage level of control input	U_{MAX}	5.0	V

The controller aims to calculate a proper control input $\mathbf{u}^*(t)$ to bring the nonlinear system (7) to the equilibrium point:

The state error vector $\mathbf{x}_e(t) = \mathbf{x}_r - \mathbf{x} = \mathbf{0}$

The input error vector $\mathbf{u}_e(t) = \mathbf{u}_r - \mathbf{u} = \mathbf{0}$

Minimizing the objective cost function (J) through a prediction horizon (T_p) As followed in (8) [50]:

$$J\big(t, \mathbf{x}_e(t), \mathbf{u}_e(t)\big) = \int_t^{t+T_p} \mathbf{x}_e^T(\tau) Q \mathbf{x}_e(\tau) + \mathbf{u}_e^T(\tau) R \mathbf{u}_e(\tau) + \frac{1}{2}\mathbf{x}_e^T(t+T_p) P \mathbf{x}_e(t+T_p) \quad (8)$$

Where, $(\mathbf{x}_e^T(\tau) Q \mathbf{x}_e(\tau) + \mathbf{u}_e^T(\tau) R \mathbf{u}_e(\tau))$ the integration of the cost function over T_p and $(\frac{1}{2}\mathbf{x}_e^T(t+T_p) P \mathbf{x}_e(t+T_p))$ is the terminal penalty which is evaluated at the final step of the optimization horizon. The Q , R and P represent the positive definite symmetric weight matrices. To track trajectory, the NMPC optimal control problem at time (t) Can be described mathematically as follows:

Find,

$$\min_{\mathbf{u}^*} J(t, \mathbf{x}_e(t), \mathbf{u}_e(t))$$

Subject to,

$$\dot{\mathbf{x}}(t) = f\big(\mathbf{x}(t), \mathbf{u}(t)\big)$$
$$\mathbf{x}(t) \in X, \big(\tau \in [t, t+T_p)\big])$$
$$\mathbf{u}(t) \in U, \big(\tau \in [t, t+T_p)\big])$$

The admissible state and control sets are identified here by the sets $X \in \mathbb{R}^3$ and $U \in \mathbb{R}^1$ as bounded by the following constraints. Operating under several physical bounds is a feature of any realistic system given by set constraints of the following:

$$x_{\min} \le x \le x_{\max}$$
$$I_{\min} \le I \le I_{\max}$$
$$U_{\min} \le u \le U_{\max}$$

The ball position state constraint is referred to by the sets (x_{min}, x_{max}), and the Maglev current saturation limit indicated by (I_{min}, I_{max}) while the input voltage control constraint is described by (U_{min}, U_{max}).

The controller aims to calculate an appropriate command input, $u(k)$, to make the system formulation operate at the equilibrium position denoted by $u_e(k) = 0, x_e(k) = 0$. It was demonstrated that the stability of predictive control was proven by using terminal penalty and constraints [51], [52] as follows:

- A continuous running cost function is considered with $f(0,0) = 0$ and $f(\mathbf{x}_e, \mathbf{u}_e) > 0$.
- Assume that the open-loop optimization problem has a definite solution at time t = 0, and that the reference control commands are constrained. i.e., $u_r < U_{max}$.
- It is assumed that $P(\cdot)$ is a continuous, differential function that meets $P(\mathbf{0}) = 0$, and $P(\mathbf{x}_e) > 0$ for all $\mathbf{x}_e \neq 0$.
- There is a terminal-state controller $\mathbf{u}_e^{\mathrm{L}}$ that meets the requirements below:

$$\dot{P}(\mathbf{x}_e) + f(\mathbf{x}_e, \mathbf{u}_e) \leq 0, \forall \mathbf{x}_e \in \Omega$$

Where the terminal-state region is denoted by Ω. Then, using the aforementioned NMPC technique, the asymptotic stability of the closed-loop system is guaranteed.

Even if P and the Ω constraint guarantees the stability of the NMPC, for real-time implementation, the constrained nonlinear optimization's computation time continues to be an issue. If an optimal solution exists, it might not be found in the limited period of time available for control. The stability analysis described above can be done without the optimal control profile, as in [53]. Any practical control profile has the potential to yield stability. It suggests that a stable closed control can be achieved by finding a feasible solution to the optimization problem. Therefore, optimization is completed if the best solution is found in the limited number of optimization stages.

A significant issue with using NMPC in real-time systems is not just stability but also computation. To address this issue, a control profile is created by the NMPC for each optimization step in this work. Only the first control signal from the control profile is received by the Maglev; all subsequent control signals are ignored. In the next step, the controller should solve again the constrained nonlinear optimization problem. But for the current optimal solution, the prior control profile provides a positive "hot start" or first solution. The optimization computation minimizes time when "hot start" is used. Additionally, using the shortest predictive control horizon possible can minimize the computation for real-time applications [54]. To further enhance adaptability, the APO is integrated to refine the predictive performance of the NMPC framework in the next section.

2.3. Optimization of the NMPC Parameters

It is important to correctly choose the values of the NMPC parameters, specifically, N, R, Q, and T_p which critical role in determining the characteristics of the system's response. Understanding these parameters is crucial to obtain a better system response. Large values of N provide a larger horizon, which generates more accurate forecasts and enhances control. However, it leads to increased computing burden which restricts the control from updating. As R increases, the controller becomes tighter, resulting in slower reactions. Due to controllers' overacting. The weighting matrices Q and R play a key role in balancing the trade-off between the system's performance (e.g., tracking error) and the control effort. Tuning these parameters plays a vital role in obtaining the best controller's response, therefore, APO is introduced in the following section.

2.4. Artificial Protozoa Optimizer (APO)

Inspired by the natural protozoa, APO, which is a metaheuristic algorithm, has been designed for engineering optimization. Within the flagellates, the representative euglena is referred to as the protozoa. The APO models the Euglena survival mechanisms, emulating their foraging, dormancy, and reproductive behaviors. This biological inspiration is foundational to the algorithm's design. In the mathematical model, the solution set is represented by the protozoa, each protozoan has an address consisting of several decision variables (dim). Three behaviors simulate the survival mechanisms of

protozoa, the first is a foraging behavior which is composed of autotrophic mode and heterotrophic mode.

When the protozoan is exposed to high light levels in the autotrophic mode, it travels toward a location with lower light intensity of the *j*th protozoan. This is mathematically modeled by:

$$X_i^{new} = X_i + f \cdot \left(X_j - X_i + \frac{1}{np} \cdot \sum_{k=1}^{np} w_a \cdot (X_{k-} - X_{k+}) \right) \odot M_f \tag{9}$$

$$X_i = \left[x_i^1, x_i^2, \ldots, x_i^{dim} \right], X_i = sort(X_i) \tag{10}$$

$$f = rand \cdot (1 + \cos(\frac{iter}{iter_{max}} \cdot \pi)) \tag{11}$$

$$np_{max} = \lfloor \frac{ps - 1}{2} \rfloor \tag{12}$$

$$w_a = e^{-\left| \frac{f(X_{k-})}{f(X_{k+}) + eps} \right|} \tag{13}$$

$$M_f[di] = \begin{cases} 1, & \text{if } di \text{ is in } rand\text{perm}(dim, \lceil dim \cdot \frac{i}{ps} \rceil) \\ 0, & \text{otherwise} \end{cases} \tag{14}$$

where X_i^{new} and X_i indicate the updated and original location of the ith protozoan, respectively. X_j is the randomly jth protozoan selection. A randomly chosen protozoan selection in the kth paired neighbor whose rank index is less than i is indicated by the symbol $X_k -$. Specifically, if X_i is X_1, X_{k-} is also set as X_1. X_{k+} refer to a randomly chosen protozoan in the kth paired neighbor, and its rank index is greater than i. Especially, if X_i is X_ns, X_{k+} is also set to X_ns, where ps is the size of population, f stands for a foraging factor, $rand$ represents random values in the [0,1] interval. $iter$ and $iter_{max}$ stand for the current and maximum iterations, respectively. np denotes the number of neighbor pairs, and np_{max} is the maximum number of np. w_a is the autotrophic mode weight factor in with eps $(2.2204e-16)$. A mapping vector (M_f) for foraging has a dimension of $(1 \times dim)$, which each element is either 0 or 1. di represents the dimensional index $di \in \{1,2, \ldots, dim\}$.

Then, in heterotrophic mode, a protozoan can absorb nutrients from its surroundings in the dark. This is can be modeled as a X_{near} is a nearby food-rich position, and:

$$X_i^{new} = X_i + f \cdot (X_{near} - X_i + \frac{1}{np} \cdot \sum_{k=1}^{np} w_h \cdot (X_{i-k} - X_{i+k})) \odot M_f \tag{15}$$

$$X_{near} = (1 \pm Rand \cdot (1 - \frac{iter}{iter_{max}})) \odot X_i \tag{16}$$

$$w_h = e^{-\left| \frac{f(X_{i-k})}{f(X_{i+k}) + eps} \right|} \tag{17}$$

$$Rand = [rand_1, rand_2, \ldots, rand_{dim}] \tag{18}$$

The second behavior is dormant behavior. Dormant behavior is a survival strategy used by protozoans to resist stressful environmental conditions. The dormancy mathematical model is as follows:

$$X_i^{new} = X_{min} + Rand \odot (X_{\max} - X_{\min}) \tag{19}$$

$$X_{min} = [lb_1, lb_2, \dots, lb_{dim}], \quad X_{max} = [ub_1, ub_2, \dots, ub_{dim}] \tag{20}$$

where X_{min} and X_{max} denote the upper and lower bound vectors. lb_{di} and ub_{di} represent the upper and lower bounds of the dith variable.

Reproduction is the last behavior; when the protozoans are of a suitable age and health. They reproduce asexually by a process called binary fission. The following is the reproduction mathematical model:

$$X_i^{new} = X_i \pm rand \cdot \left(X_{min} + Rand \odot (X_{max} - X_{min})\right) \odot M_r \tag{21}$$

$$M_r[di] = \begin{cases} 1, & \text{if } di \text{ is in } rand\text{perm}(dim, [dim \cdot rand]) \\ 0, & \text{otherwise} \end{cases} \tag{22}$$

Where M_r is a mapping vector in the reproduction process, whose size is $(1 \times dim)$, and each element is 0 or 1.

Algorithm 1: APO

Input: Initialize parameters ps, dim, np, pf_{max}, and $MaxFEs$ (maximum function evaluations).
Output: The global optima X_{gbest} and $f(X_{gbest})$.

while $FEs < MaxFEs$ **do**
  sort(X_i), $i = 1, 2, \dots, ps$;
  $pf = pf_{max} \cdot rand$; // proportion fraction;
  $\boldsymbol{Dr}_{index} = randperm(ps, [ps \cdot pf])$; // index vector of dormancy and reproduction
  for $i = 1{:}ps$ do
    if i is in Dr_{index} **then**
      if $p_{dr} > rand$ **then**
        Calculate X_i^{new} using Eq. (19); // dormancy
      else
        $M_r = zeros(1, dim)$;
        M_r[1,rand perm$(dim, [dim \cdot \text{rand}])] = 1$;
        Calculate X_i^{new} using Eq. (21); // reproduction
      end if
    else
      $M_f = zeros(1, dim)$;
      $M_f\left[1, randperm\left(dim, [dim \cdot \frac{i}{ps}]\right)\right] = 1$
      if $p_{ah} > rand$ **then**
        Calculate X_i^{new} using Eq. (9); // foraging in an autotroph
      else
        Calculate X_i^{new} using Eq. (15); // foraging in an heterotroph
      end if
    end if
    if $f(X_i^{\text{new}}) < f(X_i)$ **then**
      $X_i \leftarrow X_i^{\text{new}}$;
    else
      $X_i \leftarrow X_i$;
    end if
  end for
  $X_{gbest} = opt\{X_i\}$;
  $FEs \leftarrow FEs + ps$;
end while

The APO algorithm can be analyzed in two stages. The initialization of the population is the first stage, using Latin hypercube sampling and random sampling as the primary methods. Traditional random sampling is utilized in this proposed algorithm. Then, the fitness value of each potential solution is assessed after the initial population has been created. In the second stage, the population is

searched for iteratively over three phases. The first step in the iterative search process, known as the guiding mechanism, solves the issue of choosing suitable solutions from the population to be used as search space reference points using an ordinal selection technique. The second phase is the search operators, which imitate the distinct behavior of natural populations. The last phase is the update mechanism, which prepares the candidate solutions, and the new population for searching new generation using the fitness value-based method. The framework of APO is shown in Fig. 2. The pseudo-code of the APO algorithm is detailed below [42]:

Fig. 2. The flowchart of APO

More details and comparative analysis with other optimization techniques in [42] for validation of the effectiveness of the APO.

3. Results and Discussion

In this section, the validation of the proposed NMPC controller of the Maglev system is conducted by simulation using MATLAB 2023b. The CasADi toolbox, employing an IPORT solver, is utilized to cope with the nonlinear system model in (6). To integrate the states of the Maglev system

in the model (6), The Runge-Kutta fourth (RK4) order method is employed with max number of iterations sets at 1000 and the IPOPT convergence criterion is kept at 10^{-8}. The optimal control problem, which is specified in the CasADi toolbox, is solved using the IPOPT solver for nonlinear programming, integrated with the multiple shooting method for state integration. All the results are simulated on a personal computer with Core i7 1.80GHz CPU and 16G RAM. The Maglev system parameters are summarized in Table 1. The Maglev states' initial conditions are $x(0) = [0.004m, 0\frac{m}{s}, 0.608A]^T$.

To verify the effectiveness of the proposed NMPC controller and the improvement in the robustness of the system under uncertainties, comparison to both LQR and PID controllers due to their broadly employed in controlling a Maglev system. These comparative simulation studies are conducted according to two main simulation scenarios. The first scenario studies the NMPC compared to LQR and PID according to the Maglev parameters in Table 1 without perturbation. Uncertainties in system parameter values can significantly impact the control design. To ensure that the controller can work properly, the design should consider these uncertainties. Therefore, the second scenario measures the robustness of the NMPC in comparison with LQR and PID and indicates its proficiency to handle the 20% perturbation of Maglev parameters uncertainties. For each scenario, comparative simulation studies based on (step, sinusoidal, and square) reference trajectories are investigated. These equations represent these three trajectories:

For step: $x_r(t) = 0.009m$

For sinusoidal: $x_r(t) = 0.001\sin(0.6\pi t) + 0.009$

For square: $x_r(t) = 0.001\,\mathrm{square}(0.6\pi t) + 0.009$

To guarantee a fair comparison, the APO optimization algorithm is utilized to tune the NMPC, LQR, and PID parameters. It runs in several iterations to minimize the cost function of each controller with different bounds. It is also crucial to select the proper cost function or performance indices that affect the APO speed in determining an optimal solution for best system performance. Two performance indexes are used in this paper namely Integral of Absolute Error (IAE) and Integral of Squared Error (ISE). IAE is defined as $\int_{t_1}^{t_2}|\boldsymbol{e(t)}|\boldsymbol{dt}$ while ISE is defined as $\int_{t_1}^{t_2}\boldsymbol{e(t)^2dt}$, where $\boldsymbol{e(t)}$ is the ball position error, and $\boldsymbol{t}$ is the interval of $t_1, t_2 \in 0, 3$ for step reference trajectory and $t_1, t_2 \in 0, 10$ for both sinusoidal and square reference trajectories. Due to the nonlinearity of the Maglev system, the potential of multi-local optimal is considerable which increases the difficulty of selecting the proper APO parameters. These parameters, such as the maximum iteration, population size, and bounds, have a significant impact on the rate of obtaining the optimal solution. The identification of the APO parameters is dependent on personal experience and trial and error as this is a novel application of APO optimization. Consequently, the APO parameters are set to 50 and 30 for max number of iterations and the population size respectively. In terms of upper and lower bounds, Table 2 shows the bounds for the NMPC, LQR, and PID.

Table 2. Upper and Lower bounds of the tuned parameters

Controller	The bounds of the tuned gains	Values
NMPC	$X_{min} = [Q_{1,1}, Q_{2,2}, Q_{3,3}, R, T_P, N]$	[1e7,10,10,1,0.001,0]
	$X_{Max} = [Q_{1,1}, Q_{2,2}, Q_{3,3}, R, T_P, N]$	[1e12,1e4,1e4,25,0.003,40]
LQR	$X_{min} = [k_1, k_2, k_3]$	[0,0,0,0.01]
	$X_{Max} = [k_1, k_2, k_3]$	[1000,1000,1000,100]
PID	$X_{min} = [k_p, k_i, k_d]$	[0,0,0,0.01]
	$X_{Max} = [k_p, k_i, k_d]$	[100,100,100,10]

All the aforementioned APO parameters are utilized to optimize the controllers' gains, Table 3 demonstrates NMPC, LQR, and PID best-tuned gains.

3.1. The First Scenario: Tracking Performance Without Perturbation

In this scenario, the three aforementioned trajectories are used to examine the controllers' performance of reference trajectory tracking without any perturbation in Maglev parameters. For the step reference trajectory, the LQR shows a slightly shorter rise time versus NMPC and PID of $46ms$, $57.1ms$, and $57.5ms$ respectively. However, NMPC shows fast convergence to the reference step trajectory with no overshoot and short settling time. It effectively minimizes the steady-state error after a short transient response, leading to better tracking as shown in Fig. 3. PID has a larger overshoot and slower settling time, indicating that it cannot handle sharp transitions such as step inputs as effectively as NMPC. Regarding the NMPC computational efficiency, the average computing time is $0.039\ sec$.

Table 3. Controllers' tuned parameters values

Controller	Parameter	Value
NMPC	Q	$\begin{bmatrix} 8.3964e11 & 0 & 0 \\ 0 & 2.7590e03 & 0 \\ 0 & 0 & 246.7660 \end{bmatrix}$
	N	10
	R	1.5426
	T_p	1.0000e-3
LQR	$[k_1, k_2, k_3]$	[329.0246, 5.7941, 0.8931]
PID	$[k_p, k_i, k_d]$	[1.5989e3, 2000, 40.9427]

In the same context, the NMPC tracking performance is more efficient at tracking more challenging trajectories such as sine and square reference trajectories. Concerning sine reference trajectory with amplitude of $0.001\ rad$ and frequency of $0.3\ Hz$ for period of $10\ sec$, the NMPC in Fig. 4 demonstrates a better tracking to the reference sin trajectory than other controllers. As observed in Fig. 4, the NMPC provides smoother and more accurate tracking of the sine wave, with minimal deviation (steady state error between the reference and the measured position. The PID controller also demonstrates good performance, but it slightly lags in terms of error minimization compared to NMPC. LQR demonstrates the worst performance among the three controllers, with significant overshoot and a clear inability to track the reference precisely. is very large in LQR than PID and NMPC while NPMC offers too smaller deviation than others, especially in rising and falling intervals.

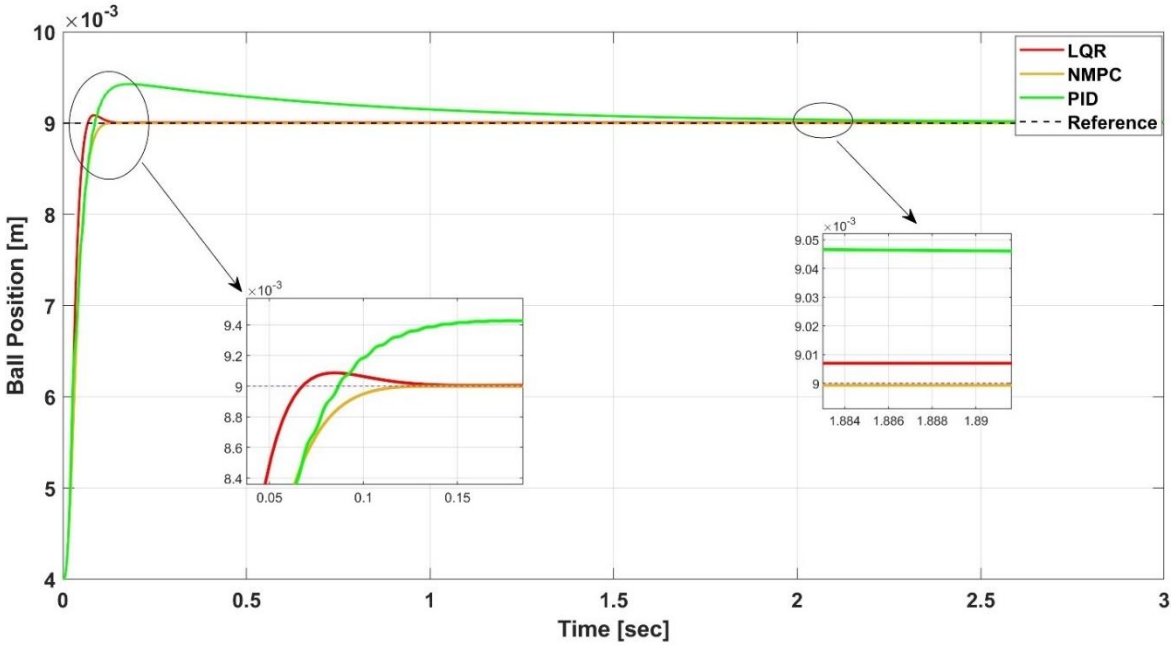

Fig. 3. Step trajectory tracking response without perturbation

The most challenging trajectory is square. With the same amplitude and frequency of sine trajectory for a period of 10 sec, the NMPC controller has clear superiority in following the square wave trajectory, showing minimal overshoot and fast convergence to the reference in comparison with LQR and PID, especially in rising and falling periods as shown in Fig. 5. The NMPC is capable of handling sudden changes in the trajectory, demonstrating its predictive ability to cope with nonlinearities and unexpected transitions. 0.041 sec and 0.063 sec are the average computed time of the NMPC computational efficiency for both Sine and square trajectories respectively. For all three trajectories, the NMPC controller adapts well to the nonlinear dynamics of the magnetic levitation system.

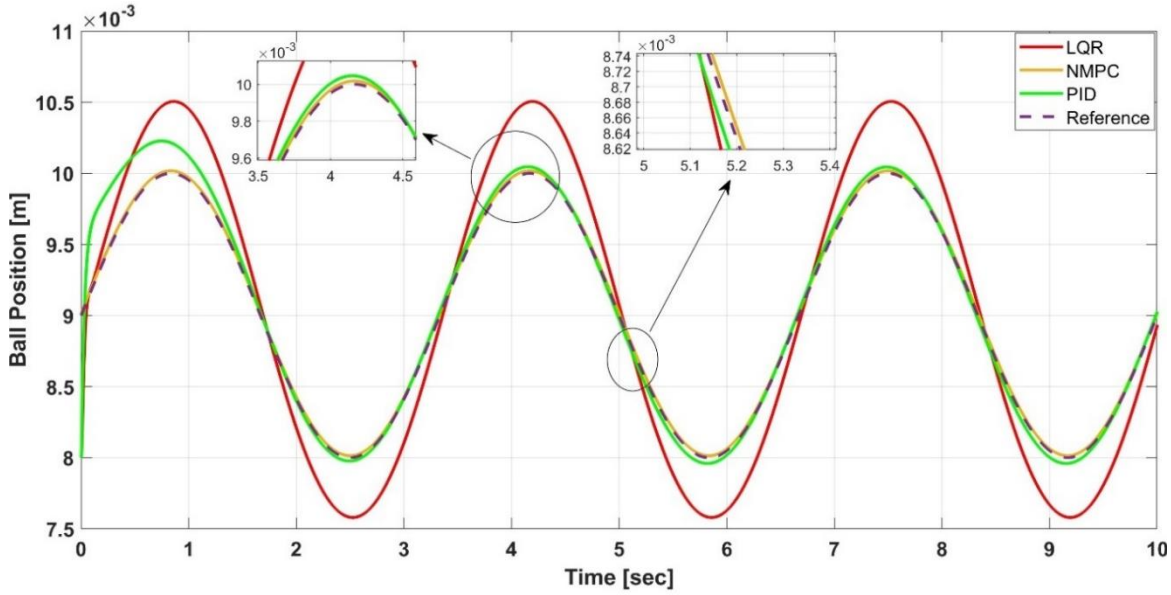

Fig. 4. Sine trajectory tracking response without perturbation

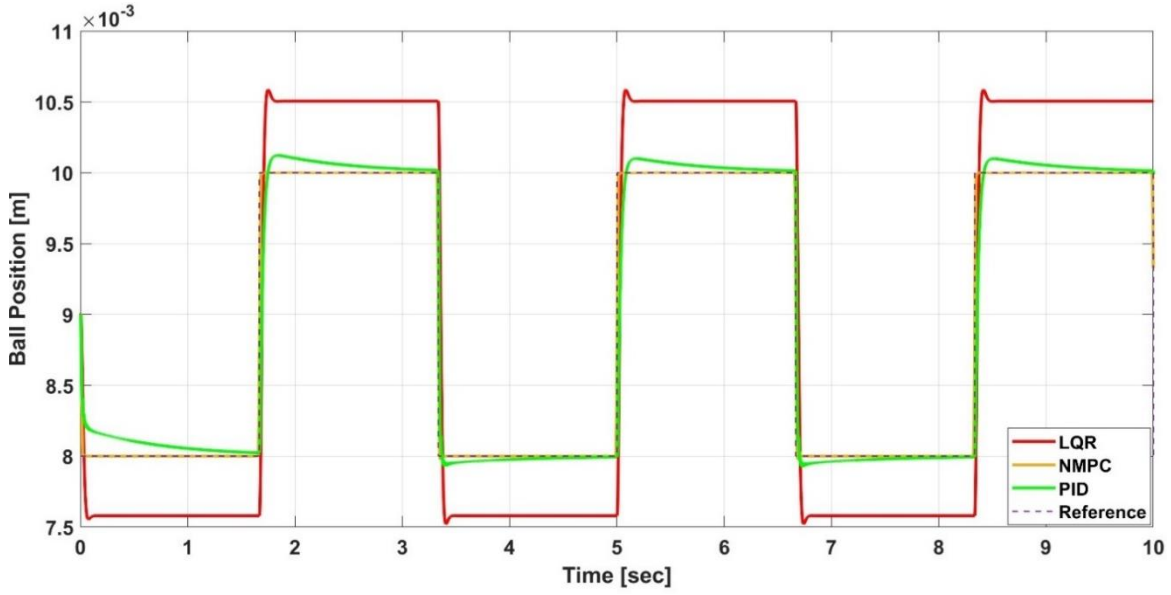

Fig. 5. Square trajectory tracking response without perturbation

3.2. The Second Scenario: Robustness Validation in the Presence of Perturbation

In this scenario, the three trajectories are applied to the Maglev system with the parameters perturbation. The values of Maglev parameters including f_{emP1},f_{emP2}, f_{P1}, f_{P2}, k, c are changed by 20% to evaluate the controllers' robustness performance. In Fig. 6, Fig. 7, Fig. 8, the LQR cannot

follow the trajectories due to its sensitivity to any change in the system, the effectiveness of its performance significantly depends on the precise system model. In contrast, PID provides better tracking trajectories and a better rise time of 49.4 ms for step tracking, but it still has an overshoot and larger deviation than NMPC.

However, the NMPC controller shows more efficient tracking performance and its ability to handle nonlinearity and constraints makes it the most robust in the presence of perturbations, providing a smoother and more accurate control response compared to other controllers. In Fig. 6, the NMPC offers 57 ms rise time with no overshoot and deviation for step trajectory. In Fig. 7, better tracking has shown with smaller steady-state error than other controllers, particularly in rising and falling intervals. The most challenging case is in Fig. 8, the NMPC provides superior tracking for reference square trajectories with no deviation of 64.9 ms as an average computed time. The average calculated time of the NMPC for step, sine, and square trajectories is 0.040 sec, 0.0414 sec, and 0.0649 sec respectively.

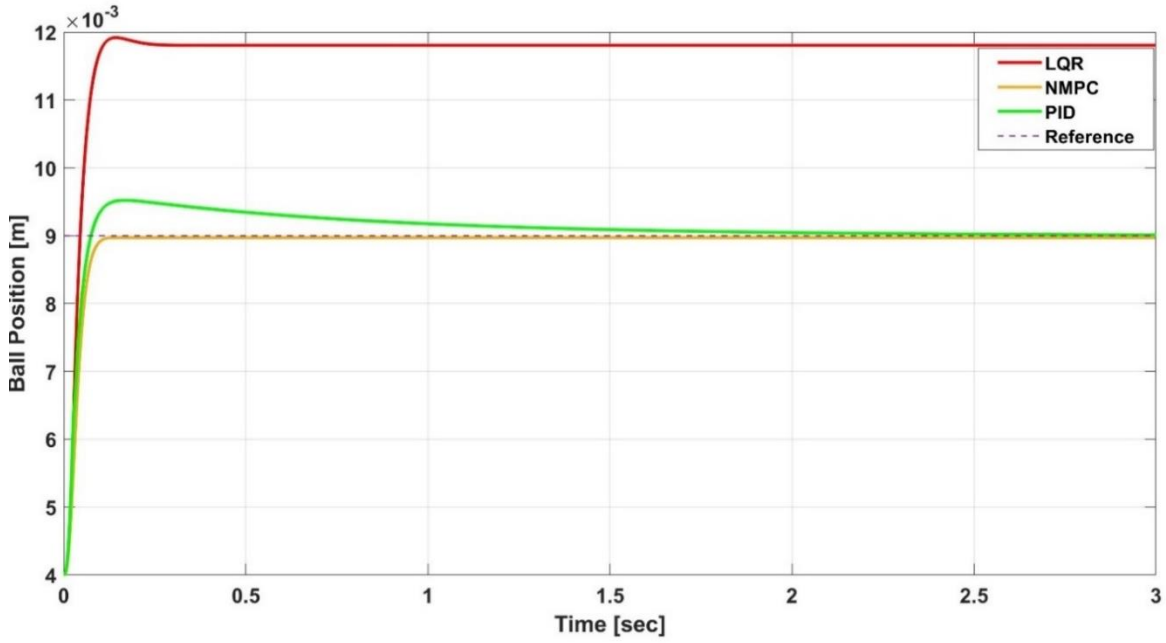

Fig. 6. Step trajectory tracking response with perturbation

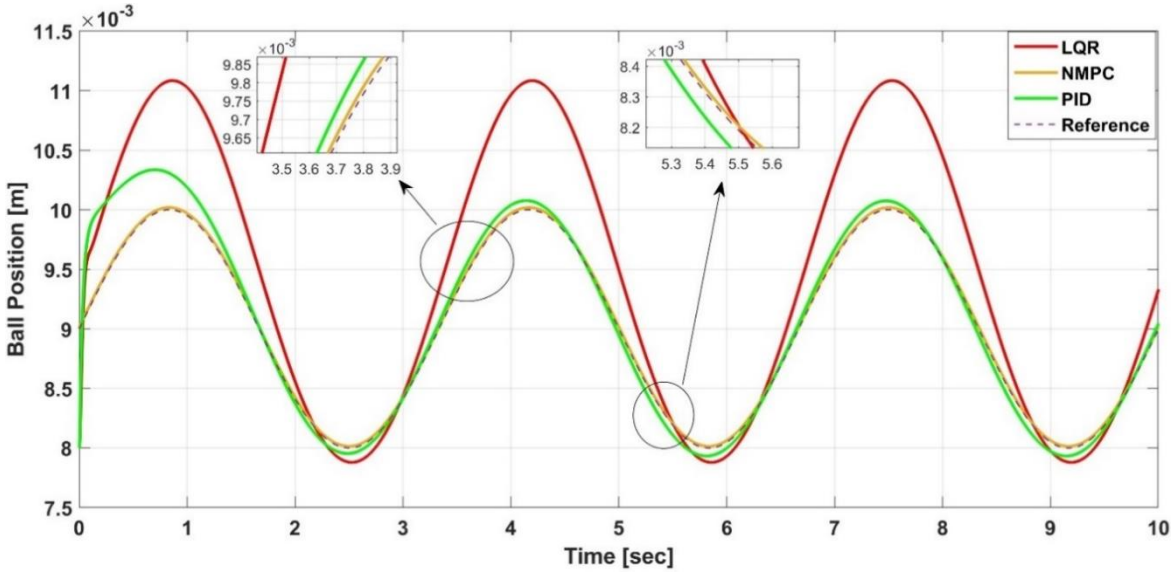

Fig. 7. Sin trajectory tracking response with perturbation

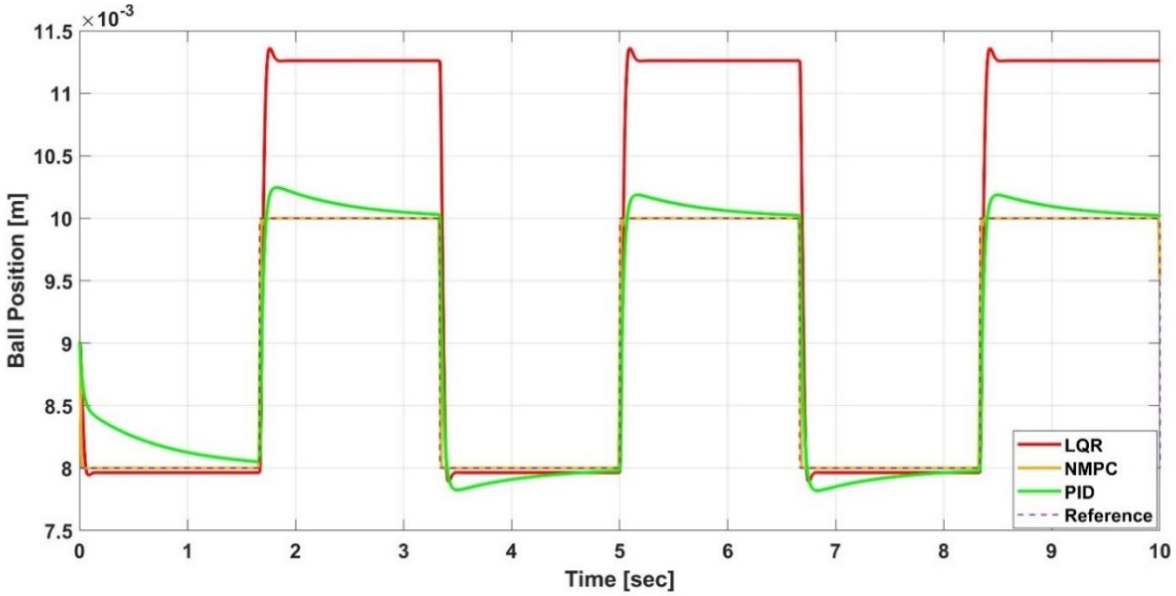

Fig. 8. Square trajectory tracking response with perturbation

3.3. Tracking Performance Indices

The comparative study of this work is also supported by Table 4 and Table 5 which consist of numerical values of assessing the NMPC, LQR, and PID controllers' effort. Two performance indices, including ISE and IAE, are indicated for controllers' evaluation. Table 4 highlights the values of the ISE of the NMPC, LQR, and PID for all three trajectories with and without perturbations. The NMPC demonstrates superior performance with lower ISE values across all input types (Sine, Square, and Step) with minimal divergence compared with LQR and PID. Even under perturbation, NMPC still maintains relatively low ISE values across all inputs, showing robustness against external disturbances. In the same context, Table 5 demonstrates the raw numbers of the IAE which indicates that NMPC has the smallest IAE compared with other controllers. In other words, IAE illustrates that NMPC reduces the total accumulated error over time including steady-state error with minimal oscillation. The NMPC shows only a slight increase in IAE with perturbation, particularly for Square and Step inputs, indicating good robustness. For both tables, PID also shows good performance in following the three reference trajectories but it still needs to be improved, while the worst performance was for LQR. This analysis highlights NMPC's strengths in handling nonlinearities and disturbances in Maglev systems, emphasizing its suitability as a control strategy in applications with similar dynamic challenges.

Table 4. ISE performance numerical values

Controller		$ISE = \int_{t_1}^{t_2} e(t)^2 dt$		
		Sine	**Square**	**Step**
Without perturbation	NMPC	2.6352e-6	1.1291e-4	1.5691e-7
	LQR	2.3967e-4	2.9451e-2	5.9171e-7
	PID	5.2016e-6	7.2945e-4	6.6726e-5
With (20%) perturbation	NMPC	2.7463e-6	1.1558e-4	1.6894e-7
	LQR	4.4458e-2	3.9310e-1	3.9863e-2
	PID	7.8991e-6	9.2426e-4	1.8810e-6

However, NMPC with APO is computationally intensive, which can be a challenge in real-time applications, especially if hardware resources are limited. Real-time implementation challenges

include practical issues such as sensor noise, actuation delays, and physical constraints that could impact performance in an actual Maglev setup, requiring additional compensations or adaptations.

Table 5. IAE performance numerical values

Controller		$IAE = \int_{t_1}^{t_2} \lvert e(t) \rvert dt$		
		Sine	**Square**	**Step**
Without perturbation	NMPC	1.5943e-4	7.1501e-4	2.4153e-5
	LQR	3.1214e-3	4.3182e-2	1.5910e-4
	PID	1.7081e-3	2.2013e-3	6.4891e-3
With (20%) perturbation	NMPC	1.6831e-4	7.3413e-4	2.5913e-5
	LQR	4.5031e-1	4.8951e-1	5.9761e-1
	PID	5.8762e-3	7.4061e-3	2.6191e-3

4. Conclusion

In this paper, a novel integration of the Artificial Protozoa Optimizer (APO) algorithm with the Nonlinear Model Predictive Control (NMPC) framework was introduced for uncertainty, nonlinear, and unstable Maglev systems. A comparative study with LQR and PID has been conducted to show the superiority of the NMPC controller. The APO was utilized to optimize the tuning parameters of the NMPC, LQR, and PID controllers by minimizing the cost function which resulted in minimal tracking error and improved the system's robustness. Three reference trajectories (step, sine, and square) were used to examine the controllers with and without Maglev parameters perturbation. The nonlinearity of the Maglev system has been solved using the IPORT solver within the CasADi toolbox in MATLAB. Aligned with these, two performance indices, including IAE and ISE, were introduced to evaluate the effectiveness of the NMPC, LQR, and PID controllers. MATLAB simulation results verified that the NMPC has shown superiority in tracking all three trajectories over other controllers. It also outperformed the other controllers even though there was a 20% change in the Maglev parameters which indicated a robust tracking performance. In addition, the superiority of the NMPC was supported by lower numerical values of both IAE and ISE for both aforementioned scenarios. As future work, the proposed NMPC controller can be implemented in real-time on a physical Maglev educational device presented in Fig. 1. In addition, an adaptive nonlinear model predictive controller can be used to address system nonlinearities and real-time changes in dynamics. By utilizing NMPC's ability to handle complex nonlinearities and constraints in real time, this research opens up new possibilities for optimizing control in advanced engineering systems, significantly enhancing their safety, efficiency, and adaptability in real-world applications such as autonomous vehicles, robotics, and aerospace.

Author Contribution: All authors contributed equally to the main contributor to this paper. All authors read and approved the final paper.

Funding: his research received no external funding.

Conflicts of Interest: The authors declare no conflict of interest.

References

[1] O. Y. Ismael, M. Qasim, and M. N. Noaman, "Equilibrium optimizer-based robust sliding mode control of magnetic levitation system," *Journal Européen des Systèmes Automatisés*, vol. 54, no. 1, pp. 131–138, 2021, https://doi.org/10.18280/jesa.540115.

[2] Y. He, J. Wu, G. Xie, X. Hong, and Y. Zhang, "Data-driven relative position detection technology for high-speed maglev train," *Measurement*, vol. 180, p. 109468, 2021, https://doi.org/10.1016/j.measurement.2021.109468.

[3] A. Chaban, Z. Lukasik, M. Lis, and A. Szafraniec, "Mathematical Modeling of Transient Processes in Magnetic Suspension of Maglev Trains," *Energies*, vol. 13, no. 24, p. 6642, 2020, https://doi.org/10.3390/en13246642.

[4] D. Rohacs and J. Rohacs, "Magnetic levitation assisted aircraft take-off and landing (feasibility study – GABRIEL concept)," *Progress in Aerospace Sciences*, vol. 85, pp. 33-50, 2016, https://doi.org/10.1016/j.paerosci.2016.06.001.

[5] A. A. Ashkarran and M. Mahmoudi, "Magnetic Levitation Systems for Disease Diagnostics," *Trends in Biotechnology*, vol. 39, no. 3, pp. 311-321, 2021, https://doi.org/10.1016/j.tibtech.2020.07.010.

[6] A. Abbas *et al.*, "Design and Control of Magnetic Levitation System," *2019 International Conference on Electrical, Communication, and Computer Engineering (ICECCE)*, 2019, https://doi.org/10.1109/icecce47252.2019.8940711.

[7] B. Bidikli and A. Bayrak, "A self-tuning robust full-state feedback control design for the magnetic levitation system," *Control Engineering Practice*, vol. 78, pp. 175-185, 2018, https://doi.org/10.1016/j.conengprac.2018.06.017.

[8] A. Mughees and S. A. Mohsin, "Design and Control of Magnetic Levitation System by Optimizing Fractional Order PID Controller Using Ant Colony Optimization Algorithm," *IEEE Access*, vol. 8, pp. 116704–116723, 2020, https://doi.org/10.1109/access.2020.3004025.

[9] J. Wang, L. Zhao, and L. Yu, "Adaptive Terminal Sliding Mode Control for Magnetic Levitation Systems With Enhanced Disturbance Compensation," *IEEE Transactions on Industrial Electronics*, vol. 68, no. 1, pp. 756–766, 2021, https://doi.org/10.1109/tie.2020.2975487.

[10] A. A. Ashkarran and M. Mahmoudi, "Magnetic Levitation Systems for Disease Diagnostics," *Trends in Biotechnology*, vol. 39, no. 3, pp. 311-321, 2021, https://doi.org/10.1016/j.tibtech.2020.07.010.

[11] B. Ataşlar-Ayyıldız, O. Karahan, and S. Yılmaz, "Control and Robust Stabilization at Unstable Equilibrium by Fractional Controller for Magnetic Levitation Systems," *Fractal and Fractional*, vol. 5, no. 3, p. 101, 2021, https://doi.org/10.3390/fractalfract5030101.

[12] Muhammad Arif Seto and Alfian Ma'arif, "PID Control of Magnetic Levitation (Maglev) System," *Journal of Fuzzy Systems and Control*, vol. 1, no. 1, pp. 25-27, 2023, https://doi.org/10.59247/jfsc.v1i1.28.

[13] M. Qasim and O. Y. Ismael, "Shared Control of a Robot Arm Using BCI and Computer Vision," *Journal Européen des Systèmes Automatisés*, vol. 55, no. 1, pp. 139-146, 2022, https://doi.org/10.18280/jesa.550115.

[14] S. Kadry and V. Rajinikanth, "Design of PID controller for magnetic levitation system using Harris hawks optimization," *Jurnal Ilmiah Teknik Elektro Komputer dan Informatika*, vol. 6, no. 2, pp. 70-78, 2020, https://doi.org/10.26555/jiteki.v6i2.19167.

[15] A. Bizuneh, H. Mitiku, A. O. Salau, and K. Chandran, "Performance analysis of an optimized PID-P controller for the position control of a magnetic levitation system using recent optimization algorithms," *Measurement: Sensors*, vol. 33, p. 101228, 2024, https://doi.org/10.1016/j.measen.2024.101228.

[16] A. Winursito and G. N. P. Pratama, "LQR state feedback controller with compensator for magnetic levitation system," *Journal of Physics: Conference Series*, vol. 2111, no. 1, p. 012004, 2021, https://doi.org/10.1088/1742-6596/2111/1/012004.

[17] Y. D. Mfoumboulou and M. E. S. Mnguni, "Development of a new linearizing controller using Lyapunov stability theory and model reference control," *Indonesian Journal of Electrical Engineering and Computer Science*, vol. 25, no. 3, p. 1328, 2022, https://doi.org/10.11591/ijeecs.v25.i3.pp1328-1343.

[18] A. A. Abbas, H. Hassan Ammar, M. M. Elsamanty, "Controller Design and Optimization of Magnetic Levitation System (MAGLEV) using Particle Swarm optimization technique and Linear Quadratic Regulator (LQR)," *2020 2nd Novel Intelligent and Leading Emerging Sciences Conference (NILES)*, vol. 15, pp. 508-513, 2020, https://doi.org/10.1109/niles50944.2020.9257873.

[19] P. Vernekar and V. Bandal, "Sliding mode control for magnetic levitation systems with mismatched uncertainties using multirate output feedback," *International Journal of Dynamics and Control*, vol. 11, no. 6, pp. 2958-2976, 2023, https://doi.org/10.1007/s40435-023-01151-3.

[20] C.-L. Zhang, X.-Z. Wu, and J. Xu, "Particle Swarm Sliding Mode-Fuzzy PID Control Based on Maglev System," *IEEE Access*, vol. 9, pp. 96337-96344, 2021, https://doi.org/10.1109/access.2021.3095490.

[21] J. Jose and S. J. Mija, "Particle Swarm optimization Based Fractional Order Sliding Mode Controller For Magnetic Levitation Systems," *2020 IEEE 5th International Conference on Computing Communication and Automation (ICCCA)*, pp. 73-78, 2020, https://doi.org/10.1109/iccca49541.2020.9250823.

[22] L. Yipeng, L. Jie, Z. Fengge, and Z. Ming, "Fuzzy Sliding Mode Control of Magnetic Levitation System of Controllable Excitation Linear Synchronous Motor," *IEEE Transactions on Industry Applications*, vol. 56, no. 5, pp. 5585-5592, 2020, https://doi.org/10.1109/tia.2020.3004763.

[23] J. S. Artal-Sevil, C. Bernal-Ruiz, A. Bono-Nuez, and M. S. Penas, "Design of a Fuzzy-Controller for a Magnetic Levitation System using Hall-Effect sensors," *2020 XIV Technologies Applied to Electronics Teaching Conference (TAEE)*, vol. 272, pp. 1-9, 2020, https://doi.org/10.1109/taee46915.2020.9163711.

[24] F. Bu and J. Xu, "Predictive Fuzzy Control Using Particle Swarm Optimization for Magnetic Levitation System," *The proceedings of the 16th Annual Conference of China Electrotechnical Society*, pp. 1353-1369, 2022, https://doi.org/10.1007/978-981-19-1528-4_137.

[25] L. Dutta and D. Kumar Das, "A Linear Model Predictive Control design for Magnetic Levitation System," *2020 International Conference on Computational Performance Evaluation (ComPE)*, pp. 039-043, 2020, https://doi.org/10.1109/compe49325.2020.9200143.

[26] B. Oppeneiger *et al*., "Model predictive control of a magnetic levitation system with prescribed output tracking performance," *Control Engineering Practice*, vol. 151, p. 106018, 2024, https://doi.org/10.1016/j.conengprac.2024.106018.

[27] Z. Zhang, Y. Zhou, and X. Tao, "Model predictive control of a magnetic levitation system using two-level state feedback," *Measurement and Control*, vol. 53, no. 5–6, pp. 962–970, Apr. 2020, https://doi.org/10.1177/0020294019900333.

[28] L. E. Jumaa Alkurawy and K. G. Mohammed, "Model predictive control of magnetic levitation system," *International Journal of Electrical and Computer Engineering (IJECE)*, vol. 10, no. 6, p. 5802, 2020, https://doi.org/10.11591/ijece.v10i6.pp5802-5812.

[29] E. Salajegheh, S. Mojalal, and A. Mojarrad Ghahfarokhi, "Treatment of Bone Marrow Cancer Based on Model Predictive Control," *International Journal of Robotics and Control Systems*, vol. 1, no. 4, pp. 463–476, 2021, https://doi.org/10.31763/ijrcs.v1i4.481.

[30] J. Berberich, J. Kohler, M. A. Muller, and F. Allgower, "Linear Tracking MPC for Nonlinear Systems—Part II: The Data-Driven Case," *IEEE Transactions on Automatic Control*, vol. 67, no. 9, pp. 4406–4421, 2022, https://doi.org/10.1109/tac.2022.3166851.

[31] D. S. Acharya, B. Sarkar, and D. Bharti, "A Fractional Order Particle Swarm Optimization for tuning Fractional Order PID Controller for Magnetic Levitation Plant," *2020 First IEEE International Conference on Measurement, Instrumentation, Control and Automation (ICMICA)*, vol. 49, pp. 1-6, 2020, https://doi.org/10.1109/icmica48462.2020.9242792.

[32] S. Ekinci, D. Izci, and M. Kayri, "An Effective Controller Design Approach for Magnetic Levitation System Using Novel Improved Manta Ray Foraging Optimization," *Arabian Journal for Science and Engineering*, vol. 47, no. 8, pp. 9673-9694, 2021, https://doi.org/10.1007/s13369-021-06321-z.

[33] S. Dey, S. Banerjee, and J. Dey, "Design of an improved robust fractional order PID controller for magnetic levitation system based on atom search optimization," *Sādhanā*, vol. 47, no. 188, 2022, https://doi.org/10.1007/s12046-022-01962-8.

[34] O. Y. Ismael, M. Qasim, M. N. Noaman, and A. Kurniawan, "Salp Swarm Algorithm-Based Nonlinear Robust Control of Magnetic Levitation System Using Feedback Linearization Approach," *Proceedings of the 3rd International Conference on Electronics, Communications and Control Engineering*, pp. 58-64, 2020, https://doi.org/10.1145/3396730.3396734.

[35] D. Schlipf, D. J. Schlipf, and M. Kühn, "Nonlinear model predictive control of wind turbines using LIDAR," *Wind Energy*, vol. 16, no. 7, pp. 1107-1129, 2012, https://doi.org/10.1002/we.1533.

[36] S. V. Raković and W. S. Levine, "Handbook of Model Predictive Control," *Springer International Publishing*, 2019, https://doi.org/10.1007/978-3-319-77489-3.

[37] N. Wu, D. Li, Y. Xi, and B. de Schutter, "Distributed Event-Triggered Model Predictive Control for Urban Traffic Lights," *IEEE Transactions on Intelligent Transportation Systems*, vol. 22, no. 8, pp. 4975-4985, 2021, https://doi.org/10.1109/tits.2020.2981381.

[38] M. H. Moradi, "Predictive control with constraints, J.M. Maciejowski; Pearson Education Limited, Prentice Hall, London, 2002, pp. IX+331, price £35.99, ISBN 0-201-39823-0," *International Journal of Adaptive Control and Signal Processing*, vol. 17, no. 3, pp. 261-262, 2003, https://doi.org/10.1002/acs.736.

[39] C.-A. Bojan-Dragos, A.-I. Stinean, R.-E. Precup, S. Preitl, E. M. Petriu, "Model predictive control solution for magnetic levitation systems," *2015 20th International Conference on Methods and Models in Automation and Robotics (MMAR)*, vol. 3, pp. 139-144, 2015, https://doi.org/10.1109/mmar.2015.7283861.

[40] A. Morsi, H. S. Abbas, S. M. Ahmed, and A. M. Mohamed, "Model Predictive Control Based on Linear Parameter-Varying Models of Active Magnetic Bearing Systems," *IEEE Access*, vol. 9, pp. 23633-23647, 2021, https://doi.org/10.1109/access.2021.3056323.

[41] Z. K. Nagy and F. Allgower, "Nonlinear model predictive control: From chemical industry to microelectronics," *2004 43rd IEEE Conference on Decision and Control (CDC) (IEEE Cat. No.04CH37601)*, vol. 4, pp. 4249-4254, 2004, https://doi.org/10.1109/cdc.2004.1429419.

[42] X. Wang, V. Snášel, S. Mirjalili, J.-S. Pan, L. Kong, and H. A. Shehadeh, "Artificial Protozoa Optimizer (APO): A novel bio-inspired metaheuristic algorithm for engineering optimization," *Knowledge-Based Systems*, vol. 295, p. 111737, 2024, https://doi.org/10.1016/j.knosys.2024.111737.

[43] A. Wächter and L. T. Biegler, "Line Search Filter Methods for Nonlinear Programming: Motivation and Global Convergence," *SIAM Journal on Optimization*, vol. 16, no. 1, pp. 1-31, 2005, https://doi.org/10.1137/s1052623403426556.

[44] J. A. E. Andersson, J. Gillis, G. Horn, J. B. Rawlings, and M. Diehl, "CasADi: a software framework for nonlinear optimization and optimal control," *Mathematical Programming Computation*, vol. 11, no. 1, pp. 1-36, 2018, https://doi.org/10.1007/s12532-018-0139-4.

[45] M. Elhesasy *et al*., "Non-Linear Model Predictive Control Using CasADi Package for Trajectory Tracking of Quadrotor," *Energies*, vol. 16, no. 5, p. 2143, 2023, https://doi.org/10.3390/en16052143.

[46] J. A. E. Andersson, J. Gillis, G. Horn, J. B. Rawlings, M. Diehl, "CasADi: a software framework for nonlinear optimization and optimal control," *Mathematical Programming Computation*, vol. 11, no. 1, pp. 1–36, 2018, https://doi.org/10.1007/s12532-018-0139-4.

[47] P. Balko and D. Rosinova, "Modeling of magnetic levitation system," *2017 21st International Conference on Process Control (PC)*, 2017, https://doi.org/10.1109/pc.2017.7976222.

[48] D. Rosinová and M. Hypiusová, "Comparison of Nonlinear and Linear Controllers for Magnetic Levitation System," *Applied Sciences*, vol. 11, no. 17, p. 7795, 2021, https://doi.org/10.3390/app11177795.

[49] R. Findeisen and F. Allgower, "Stabilization using sampled-data open-loop feedback - A nonlinear model predictive control perspective," *IFAC Proceedings Volumes*, vol. 37, no. 13, pp. 579-584, 2004, https://doi.org/10.1016/s1474-6670(17)31286-7.

[50] W. B. Dunbar and R. M. Murray, "Model predictive control of coordinated multi-vehicle formations," *Proceedings of the 41st IEEE Conference on Decision and Control*, vol. 4, pp. 4631-4636, 2002, https://doi.org/10.1109/cdc.2002.1185108.

[51] L. Grüne and J. Pannek, "Nonlinear Model Predictive Control," *Nonlinear Model Predictive Control*, pp. 45-69, 2016, https://doi.org/10.1007/978-3-319-46024-6_3.

[52] D. Q. Mayne, J. B. Rawlings, C. V. Rao, P. O. M. Scokaert, "Constrained model predictive control: Stability and optimality," *Automatica*, vol. 36, no. 6, pp. 789-814, 2000, https://doi.org/10.1016/s0005-1098(99)00214-9.

[53] T. P. Nascimento, C. E. T. Dórea, and L. M. G. Gonçalves, "Nonlinear model predictive control for trajectory tracking of nonholonomic mobile robots," *International Journal of Advanced Robotic Systems*, vol. 15, no. 1, 2018, https://doi.org/10.1177/1729881418760461.

[54] O. Y. Ismael, M. Almaged, and A. I. Abdulla, "Nonlinear Model Predictive Control-based Collision Avoidance for Mobile Robot," *Journal of Robotics and Control (JRC)*, vol. 5, no. 1, pp. 142-151, 2024, https://doi.org/10.18196/jrc.v5i1.20615.